Epidemics 48 (2024) 100789

Contents lists available at ScienceDirect

Epidemics

journal homepage: www.elsevier.com/locate/epidemics

Investigation of *P. vivax* elimination via mass drug administration: A simulation study

Md Nurul Anwar [a,*], James M. McCaw [a,b], Alexander E. Zarebski [a], Roslyn I. Hickson [a,c,d,1], Jennifer A. Flegg [a,1]

[a] School of Mathematics and Statistics, The University of Melbourne, Parkville, Australia
[b] Centre for Epidemiology and Biostatistics, Melbourne School of Population and Global Health, The University of Melbourne, Parkville, Australia
[c] Australian Institute of Tropical Health and Medicine, James Cook University, Townsville, Australia
[d] CSIRO, Townsville, Australia

ARTICLE INFO

Keywords:
P. vivax elimination
Stochastic model
Hypnozoite
Relapse
Mass drug administration

ABSTRACT

Plasmodium vivax is the most geographically widespread malaria parasite. *P. vivax* has the ability to remain dormant (as a hypnozoite) in the human liver and subsequently reactivate, which makes control efforts more difficult. Given the majority of *P. vivax* infections are due to hypnozoite reactivation, targeting the hypnozoite reservoir with a radical cure is crucial for achieving *P. vivax* elimination. Stochastic effects can strongly influence dynamics when disease prevalence is low or when the population size is small. Hence, it is important to account for this when modelling malaria elimination. We use a stochastic multiscale model of *P. vivax* transmission to study the impacts of multiple rounds of mass drug administration (MDA) with a radical cure, accounting for superinfection and hypnozoite dynamics. Our results indicate multiple rounds of MDA with a high-efficacy drug are needed to achieve a substantial probability of elimination. This work has the potential to help guide *P. vivax* elimination strategies by quantifying elimination probabilities for an MDA approach.

1. Introduction

Among the five species of the *Plasmodium* parasite, *P. vivax* is the most geographically widespread and causes significant global morbidity and mortality (Antinori et al., 2012; Battle et al., 2019). *P. vivax* has emerged as the dominant species in Southeast Asia and was responsible for 46% of cases (5.2 million total) in 2022 (WHO, 2023a). An important characteristic of *P. vivax* is its ability to remain dormant in the human liver as a *hypnozoite*. *P. vivax* can remain dormant for up to a year, before reactivating and potentially causing onward transmission (Imwong et al., 2007; Thriemer et al., 2021). Relapse events (where the hypnozoites reactivate) are responsible for more than 80% of *P. vivax* infections (in the absence of radical cure treatment) (Robinson et al., 2015).

Despite the clinical significance of relapse, there is still uncertainty regarding the causes of hypnozoite reactivation. Some factors thought to be relevant include fever caused by other infections (such as *P. falciparum*), and recognition by the immune system of the same *Anopheles* specific protein (found in the salivary glands of adult female mosquitoes) (Mueller et al., 2009; Hulden and Hulden, 2011; White et al., 2014).

It can be challenging to distinguish relapse from other types of recurrent malaria, such as reinfection or recrudescence. This can be due to incomplete elimination of a blood-stage infection, often associated with treatment failure (Ghosh et al., 2020). Antimalarial drugs refer to those that clear either blood-stage or liver-stage parasites, with the specific recommended drugs depending on the parasite species.

Implementation of radical cure treatment is a part of standard case management in all *P. vivax* endemic settings. Targeting the hypnozoite reservoir is crucial in controlling or eliminating *P. vivax*, as transmission can be re-established from the reactivation of hypnozoites (White et al., 2014). The 8-aminoquinoline class of drugs, such as primaquine and tafenoquine, clear hypnozoites from the liver, and are referred to as *radical cure* drugs (Wells et al., 2010; Taylor et al., 2019; Poespoprodjo et al., 2022). The current treatment recommended by the WHO for *P. vivax* malaria is a combination of two antimalarial drugs: either chloroquine or artemisinin combination therapy (ACT) to clear parasites from the blood and either primaquine or tafenoquine to clear hypnozoites from the liver.

Mass drug administration (MDA) is a strategy used to control and eliminate malaria. MDA involves treating the entire at-risk population,

* Corresponding author.
E-mail address: nurul.anwar@unimelb.edu.au (M.N. Anwar).
[1] These authors contributed equally to this work.

https://doi.org/10.1016/j.epidem.2024.100789
Received 30 May 2024; Received in revised form 5 August 2024; Accepted 22 August 2024
Available online 31 August 2024

or a well-defined sub-population, in a location with antimalarial drugs (depending on the malaria species), regardless of whether they have symptoms or a positive malaria diagnosis (Newby et al., 2015; Hsiang et al., 2013). In a radical cure MDA intervention (for *P. vivax*), individuals are typically given a combination of two drugs in line with the WHO-recommended treatment; one drug targets the blood-stage parasites and the other targets parasites in the liver. These radical cure MDA approaches aim to reduce both the blood-stage parasites and the size of the hypnozoite reservoir. However, there are costs to indiscriminant drug administration; primaquine and tafenoquine can cause life-threatening *haemolysis* in individuals with G6PD deficiency. G6PD deficiency is an enzymopathy affecting up to 30% of individuals in malaria-endemic regions (Recht et al., 2018). Therefore, G6PD testing is recommended before administering 8-aminoquinoline.

Mathematical modelling has been widely used to understand the transmission of malaria, particularly *P. falciparum*, and the likely impact of interventions. *P. vivax* transmission differs from *P. falciparum* transmission, in that there are recurrent infections due to hypnozoite reactivation (White et al., 2014; Anwar et al., 2022; Nekkab et al., 2023; Anwar et al., 2023a). Mathematical models have been developed to study different aspects of *P. vivax* dynamics (Anwar et al., 2023b): e.g. variation in hypnozoite numbers between infectious mosquito bites, the acquisition of immunity, superinfection (multiple simultaneous infections), and the effects of treatment. Many of the mathematical models use differential equations, as more analytical methods can be brought to bear on them, relative to stochastic or agent-based models.

When exploring disease elimination scenarios, stochastic effects can be important (Henle et al., 2004; Ludwig, 1999). Furthermore, when the population size is small, or the disease is at low prevalence, a stochastic model can provide more realistic representations of the transmission dynamics than deterministic models (Allen and Burgin, 2000; Beran, 1994). We have previously modelled hypnozoite acquisition, population dynamics and *P. vivax* transmission in a deterministic multiscale framework (Anwar et al., 2022). We also modelled the effect of the drug on both hypnozoite acquisition and infection, accounting for superinfection (Anwar et al., 2023a) utilising the framework developed earlier (Anwar et al., 2022). To the best of our knowledge, no stochastic multiscale models have been developed that can consider *P. vivax* elimination while explicitly accounting for superinfection and the effects of multiple rounds of (optimally implemented) MDA on hypnozoite dynamics and *P. vivax* infection (Anwar et al., 2023b). The only agent-based model that considers detailed hypnozoite dynamics and MDA, does not consider hypnozoite variation across mosquito bites (Nekkab et al., 2023). In this paper, we implement a stochastic multiscale model, which is based on our previous work (Anwar et al., 2023a; Mehra et al., 2022) and demonstrate how this model can be used to estimate the probability of *P. vivax* elimination under multiple MDA rounds.

2. Methods

2.1. Transmission model

We partition the human population based on individuals' *P. vivax* status as described in Anwar et al. (2023a). Let S, I, and L represent the number of people in the human population who are *susceptible* to infection with no hypnozoites, *blood-stage infected* (with or without hypnozoites), and those who are *blood-stage negative but hypnozoite positive*, respectively.

While members within the I or L class may differ in the number of hypnozoites they have, we do not track this in our representation of the population. Instead, we model the distribution of the number of hypnozoites across the individuals in each class. This distribution is based on a stochastic, within-host model (Mehra et al., 2022). We assume a constant size for the human population, i.e. $T_h = S + I + L$ is constant, where T_h is the human population size.

Let S_m, E_m and I_m represent the number of mosquitoes that are susceptible, exposed, and infectious, where $S_m,\ E_m,\ I_m \in \{0, 1, 2, \ldots, T_m\}$ and $S_m + E_m + I_m = T_m$. T_m is not fixed and varies seasonally due to a varying birth rate, $\theta(t)$, given by

$$\theta(t) = g\left(1 + \eta\cos\left(\frac{2\pi t}{365}\right)\right), \tag{1}$$

where g is the baseline mosquito birth (and death) rate and $\eta \in [0\ \ 1)$ is the seasonal amplitude. Note that only the individuals in the I compartment are infectious to mosquitoes. A schematic of the stochastic multiscale model is provided in Fig. 1. Table 1 describes the possible compartment transitions and their associated rates, and Table 2 describes the value and source of the parameter values used.

Upon being bitten by an infected mosquito, humans in the S and L compartments transition to the blood-stage infected compartment (I). The rate at which individuals from S and L transition to I is $\lambda(t) = abI_m/T_h$, where a is the mosquito biting rate and b is the probability of transmission from a mosquito bite.

To capture the hypnozoite dynamics and the variation of hypnozoites within individuals at the population level, we embed the within-host model of Mehra et al. (Mehra et al., 2022) into our model to capture the additional structure within the I and L compartments. We use the mean-field approximation to obtain the probability distribution of hypnozoites within individuals. The mean-field approximation provides a deterministic approximation for a Markov chain by using the functional law of large numbers (Kurtz, 1970). It is fast to compute since one only needs to compute the model once to understand the mean behaviour of the system. Here, we consider the short latency case, with 100% probability of becoming blood-stage infected after an infectious bite ($p_{\text{prim}} = 1$), where hypnozoites can activate immediately following establishment (Mehra et al., 2022). We assume the number of hypnozoites introduced by an infectious bite follows a geometric distribution with mean ν and the dynamics of each hypnozoite are independent and identically distributed. Let H, A, C, and D represent states of establishment, activation, clearance (removal after activation) and death (removal before activation) of a hypnozoite, respectively. Each hypnozoite has two possible final states: death before activation (D); or clearance after activation (C). Furthermore, let $N_f(t)$ denote the number of hypnozoites in states $f \in F := \{H, A, C, D\}$ at time t and $N_P(t),\ N_{PC}(t)$ denote the number of ongoing and cleared primary infections (an infection from an infectious mosquito bite), respectively, at time t. We assume that the dynamics of each hypnozoite are independent and identically distributed, and each mosquito bite establishes a number of hypnozoites that is geometrically distributed with mean, ν (these and related assumptions are further explained in Supplementary materials Section 1.1). We then calculate the probability generating function (PGF) of $N_f,\ f \in F' := \{H, A, C, D, P, PC\}$ for the distribution of hypnozoites at time t for different states (see Supplementary Material for details).

In the absence of MDA treatment, we assume that individuals recover naturally. That is, individuals in I transition to S at rate $p_1(t)\gamma$. Here, γ is the natural recovery rate from a blood-stage infection and $p_1(t)$ is the probability that a blood-stage infected individual has no hypnozoites and only a single blood-stage infection (i.e. they do not have a superinfection). The derivation of p_1 is given in the Supplementary Material and results in

$$p_1(t) = \frac{P\big(N_A(t) + N_P(t) = 1 | N_H(t) = 0\big)P(N_H(t) = 0)}{1 - P\big(N_A(t) + N_P(t) = 0\big)}, \tag{2}$$

where $N_H(t),\ N_A(t),$ and $N_P(t)$ are the number of established hypnozoites in the liver, the number of relapses (that is, hypnozoites that have reactivated), and the number of primary infections, respectively. Individuals transition from I to L at the rate $p_2(t)\gamma$. Again, γ is the rate of natural recovery from a blood-stage infection, and now $p_2(t)$ is the probability that a blood-stage infected individual has at least one hypnozoite and only one blood-stage infection (i.e. they do not have a

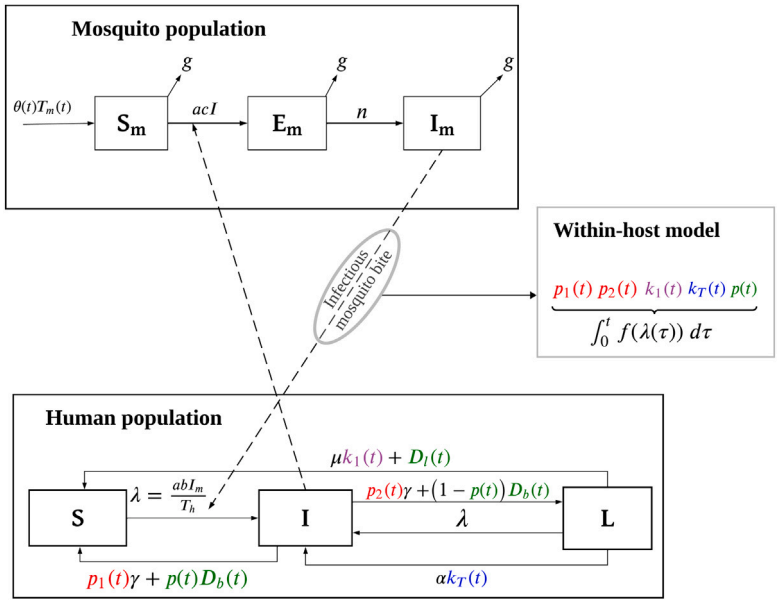

Fig. 1. Schematic illustration of the multiscale model with treatment. The left (top and bottom) part of the schematic demonstrates the transmission dynamics between the human and mosquito populations. S, I and L represent the number of humans that are susceptible with no hypnozoites, blood-stage infected (with or without hypnozoites), and blood-stage negative but hypnozoite positive, respectively. S_m, E_m and I_m represent the number of susceptible, exposed and infectious mosquitoes, respectively. The right part of the schematic demonstrates how the within-host model has been embedded within the population scale model. The within-host model takes into account the history of infective bites (as a function of $\lambda(t)$) and calculates the probability of individuals in the I compartment having no hypnozoites and one blood-stage infection ($p_1(t)$), individuals in the I compartment having at least one hypnozoite and one blood-stage infection ($p_2(t)$), individuals in the L compartment having one hypnozoite ($k_1(t)$), the expected size of the hypnozoite reservoir ($k_T(t)$), and the probability of individuals in I having no hypnozoites ($p(t)$) at any given time t as a function of the force of reinfection, $\lambda(t)$. We account for superinfection through the parameters $p_1(t)$ and $p_2(t)$. The functions $D_b(t)$ and $D_l(t)$ capture the effect of treatment when implemented. Other parameters are defined in Table 2.

Table 1
Table of transition rates and stoichiometries for the stochastic multiscale model.

Event	Event type	Stoichiometries	Rate
1	Infection of individual in S compartment	$(S,\ I,\ L,\ S_m,\ E_m,\ I_m) \to (S-1,\ I+1,\ L,\ S_m,\ E_m,\ I_m)$	$abSI_m/T_h$
2	Infection of individual in L compartment	$(S,\ I,\ L,\ S_m,\ E_m,\ I_m) \to (S,\ I+1,\ L-1,\ S_m,\ E_m,\ I_m)$	$abLI_m/T_h$
3	Relapse of individual in L compartment	$(S,\ I,\ L,\ S_m,\ E_m,\ I_m) \to (S,\ I+1,\ L-1,\ S_m,\ E_m,\ I_m)$	$\alpha k_T(t)L$
4	Death of the last hypnozoite in individual in L compartment	$(S,\ I,\ L,\ S_m,\ E_m,\ I_m) \to (S+1,\ I,\ L-1,\ S_m,\ E_m,\ I_m)$	$\mu k_1(t)L$
5	Natural recovery from I compartment without hypnozoites	$(S,\ I,\ L,\ S_m,\ E_m,\ I_m) \to (S+1,\ I-1,\ L,\ S_m,\ E_m,\ I_m)$	$p_1(t)\gamma I$
6	Natural recovery from I compartment (with hypnozoites)	$(S,\ I,\ L,\ S_m,\ E_m,\ I_m) \to (S,\ I-1,\ L+1,\ S_m,\ E_m,\ I_m)$	$p_2(t)\gamma I$
7	Recovery from I compartment (without hypnozoites) due to radical cure	$(S,\ I,\ L,\ S_m,\ E_m\ I_m) \to (S+1,\ I-1,\ L,\ S_m,\ E_m,\ I_m)$	$p(t)D_b(t)I$
8	Recovery from I compartment (with hypnozoites) due to radical cure	$(S,\ I,\ L,\ S_m,\ E_m\ I_m) \to (S,\ I-1,\ L+1,\ S_m,\ E_m,\ I_m)$	$(1-p(t))D_b(t)I$
9	Recovery from L compartment due to radical cure	$(S,\ I,\ L,\ S_m,\ E_m\ I_m) \to (S+1,\ I,\ L-1,\ S_m,\ E_m,\ I_m)$	$D_l(t)L$
10	Birth of mosquitoes	$(S,\ I,\ L,\ S_m,\ E_m,\ I_m) \to (S,\ I,\ L,\ S_m+1,\ E_m,\ I_m)$	$\theta(t)T_m(t)$
11	Mosquito exposure to sporozoites	$(S,\ I,\ L,\ S_m,\ E_m,\ I_m) \to (S,\ I,\ L,\ S_m-1,\ E_m+1,\ I_m)$	acS_mI/T_h
12	Mosquito becomes infectious	$(S,\ I,\ L,\ S_m,\ E_m,\ I_m) \to (S,\ I,\ L,\ S_m,\ E_m-1,\ I_m+1)$	nE_m
13	Death of susceptible mosquito	$(S,\ I,\ L,\ S_m,\ E_m,\ I_m) \to (S,\ I,\ L,\ S_m-1,\ E_m,\ I_m)$	gS_m
14	Death of exposed mosquito	$(S,\ I,\ L,\ S_m,\ E_m,\ I_m) \to (S,\ I,\ L,\ S_m,\ E_m-1,\ I_m)$	gE_m
15	Death of infectious mosquito	$(S,\ I,\ L,\ S_m,\ E_m,\ I_m) \to (S,\ I,\ L,\ S_m,\ E_m,\ I_m-1)$	gI_m

superinfection.) As derived in the Supplementary Material, the equation for p_2 is

$$p_2(t) = \frac{P\big(N_A(t)+N_P(t)=1\big)}{1-P\big(N_A(t)+N_P(t)=0\big)} - p_1(t). \tag{3}$$

Furthermore, individuals transition from L to S at rate $\mu k_1(t)$ where μ is the hypnozoite death rate and $k_1(t)$ is the probability that an individual in the L compartment has only a single hypnozoite:

$$k_1(t) = \frac{P\big(N_H(t)=1|N_A(t)=N_p(t)=0\big)}{1-P\big(N_H(t)=0|N_A(t)=N_P(t)=0\big)}. \tag{4}$$

The rate individuals transition from L to I is $\alpha k_T(t)$, where α is the hypnozoite activation rate and $k_T(t)$ is the expected size of the hypnozoite reservoir within an individual in the L compartment. The expected size of the hypnozoite reservoir is given by

$$k_T = \sum_{i=1}^{\infty} ik_i = \Big(\frac{\mathbb{E}\left[N_H(t)|N_A(t)=N_P(t)=0\right]}{1-P\big(N_H(t)=0|N_A(t)=N_P(t)=0\big)}\Big), \tag{5}$$

where $\mathbb{E}\left[N_H(t)|N_A(t)=N_P(t)=0\right]$ is the expected size of the hypnozoite reservoir in an uninfected individual (not in compartment I).

2.2. Treatment

We assume drug treatment is administered at times $t = s_1, s_2, \ldots, s_{N_{\text{MDA}}}$, where N_{MDA} is the total number of MDA rounds. Here, for model simplicity, we assume that the treatment coverage is 100%. Upon administration of the radical cure treatment, we assume the following: the blood-stage infections in an individual are instantaneously cleared with probability p_{blood}; and each hypnozoite in the liver dies (independently) with probability p_{rad}. We assume that the effect of the radical cure drug on blood-stage infection is independent of its effect on hypnozoites. Therefore, whenever radical cure treatment is administered, individuals in the I compartment recover with probability p_{blood} and, depending on the size of the hypnozoite reservoir, transition to compartment (S) or compartment (L). We define a probability $p(t)$, that a blood-stage

Table 2
Definitions, values and sources for model parameters. The parameter ranges indicated in square brackets were used in the sensitivity analysis.

Symbol	Definition	Value/s	Source
a	Biting rate of mosquitoes	80 year^{-1}	Garrett-Jones (1964)
b	Transmission probability: mosquito to human	0.5	Smith et al. (2010)
c	Transmission probability: human to mosquito	0.23	Bharti et al. (2006)
$\theta(t)$	Mosquito birth rate (seasonal)	Time-varying	Eq. (1)
g	Baseline mosquito birth (and death) rate	0.1 day^{-1}	Gething et al. (2011)
η	Seasonal amplitude	0.1	Assumed
T_h	Population size of human	10,000	Assumed
$T_m(t)$	Population size of mosquito	Seasonal	Modelled
$T_m(0)$	Initial number of mosquito population	Calculated	$T_m(0) = m_0 T_h$
m_0	Initial mosquito to human ratio	Varied	
n	Rate of mosquito sporogony	1/12 days^{-1}	Gething et al. (2011)
γ	Recovery rate from I compartment	1/60 day^{-1}	Collins et al. (2003)
α	Hypnozoite activation rate	1/332 day^{-1} [0, 1/100]	White et al. (2014)
μ	Hypnozoite death rate	1/425 day^{-1} [0, 1/100]	White et al. (2014)
ν	Average number of hypnozoites per mosquito bite	8.5	White et al. (2014)
$\lambda(t)$	Force of reinfection	Calculated	$\lambda(t) = abI_m/T_H$
$p(t)$	Probability that individual in I has no hypnozoites within liver	Calculated	Eq. (6)
$p_1(t)$	Probability that individual in I has no hypnozoites and $MOI = 1$	Calculated	Eq. (2)
$p_2(t)$	Probability that individual in I has hypnozoites and $MOI = 1$	Calculated	Eq. (3)
$k_1(t)$	Probability that individual in L has 1 hypnozoite within liver	Calculated	Eq. (4)
$k_T(t)$	Average number of hypnozoites within liver for individual in L	Calculated	Eq. (5)
p_{blood}	Probability that ongoing blood-stage infections are cleared instantaneously due to radical cure	0.9 [0.5, 1]	Assumed
p_{rad}	Probability that hypnozoites dies instantaneously due to radical cure	0.9 [0.5, 1]	Brito et al. (2024)
$D_b(t)$	Clearance rate of blood-stage parasite due to radical cure	Calculated	Eq. (7)
$D_l(t)$	Clearance rate of liver-stage parasite (hypnozoite) due to radical cure	Calculated	Eq. (8)
N_{MDA}	Total number of MDA rounds	Varied	

infected individual has no hypnozoites in the liver immediately after the treatment:

$$p(t) = P\big(N_H(t) = 0 | N_A(t) > 0 \cup N_P(t) > 0\big) = \frac{P(N_H(t) = 0) - P\big(N_H(t) = N_A(t) = N_P(t) = 0\big)}{1 - P\big(N_A(t) = N_P(t) = 0\big)}. \quad (6)$$

Assuming there is an MDA at time t, blood-stage infected individuals will transition to the susceptible compartment (S) with probability $p(t)D_b(t)$ and will transition to the L compartment with probability $(1 - p(t))D_b(t)$. Furthermore, individuals in the L compartment will transition to the compartment (S) at an impulse $D_l(t)$ due to the radical cure. The equations for $D_b(t)$ and $D_l(t)$ can be written as

$$D_b(t) = p_{\text{blood}} \sum_{j=1}^{N_{\text{MDA}}} \delta_D(t - s_j), \quad (7)$$

$$D_l(t) = \big\{k_1(t)p_{\text{rad}} + k_2(t)p_{\text{rad}}^2 + \cdots\big\} \sum_{j=1}^{N_{\text{MDA}}} \delta_D(t - s_j), \quad (8)$$

where $\delta_D(\cdot)$ is the Dirac delta function and $s_j,\ j = 1, 2, \ldots, N_{\text{MDA}}$, are the MDA administration times and $k_i,\ i = 1, 2, \ldots$ are the probability that individuals in the L compartment have i hypnozoites within the liver. That is, the functions $D_b(t)$ and $D_l(t)$ take effect only at the MDA administration time. As each hypnozoite will die with the probability p_{rad} due to the effect of radical cure drug, the liver-stage clearance impulse, $D_l(t)$, depends on how many hypnozoites are present in the liver. The time-dependent probabilities $p(t),\ p_1(t),\ p_2(t),\ k_1(t)$, and $k_T(t)$ depend on the history of past infections (see Supplementary Material).

2.3. Objective of the study

Our primary objective here is to study the effect of a radical cure-based MDA intervention on the probability of *P. vivax* elimination. We construct an optimisation problem to obtain the optimal MDA timings reflecting that our objective is elimination. Since we use the mean-field approximation of the within-host model, here we optimise the deterministic version of the model to avoid the added complexity. Though disease elimination may happen when prevalence is at a low level, for *P. vivax*, a low number of blood-stage infections may not be sufficient to guarantee elimination due to the re-established infection by the hypnozoite reservoir. Therefore, we define elimination to have occurred when there is no infection in the human and mosquito populations, i.e., $I + L + E_m + I_m = 0$. When seasonality is not considered, the time of the first MDA, s_1, can be considered arbitrary (as long as the dynamics have reached an equilibrium). However, when considering seasonality in the mosquito population, the time of the first MDA round is no longer arbitrary, as the dynamics display periodic oscillations around the mean annual prevalence. We define the prevalence as the proportion of the population in the I compartment. We further define x_0 to be the interval between the first MDA round and the most recent peak prevalence (of blood-stage infections). Formally, the optimisation problem can be written as

$$\underset{x_0, x_1, \ldots, x_{N_{\text{MDA}}-1}}{\text{minimise}} \quad Z$$
$$\text{s.t.} \quad x_1,\ x_2,\ \ldots,\ x_{N_{\text{MDA}}-1} > 0,\ x_0 \geq 0 \text{ and } \sum x_i \leq t_{max},$$

where

$$Z = \int_{s_1}^{t_{max}} \Big(I(t) + L(t) + E_m(t) + I_m(t)\Big) dt$$

is the objective function and the $x_i,\ i = 1, 2, \ldots, N_{\text{MDA}} - 1$ are the intervals between MDA rounds. That is, our objective is to minimise the area under the curve as keeping the total infection low for a longer duration (instead of at an instant) will encourage disease extinction (for the stochastic model). We minimise the objective function across a six-year period, starting from the first MDA round (e.g., $t_{max} = 6$ years).

Fig. 2 summarises the optimal timing of each of the MDA rounds (up to 4 rounds) for varying initial mosquito to human ratios m_0 (hence prevalence), under the (deterministic) model with seasonal dynamics. This figure is produced with the deterministic version of the stochastic model as in Anwar et al. (2023a) and shows that the optimal timing of the MDA does not vary considerably as a function of the initial mosquito to human ratio, m_0, especially when one (Fig. 2A) and two (Fig. 2B) MDA rounds are under consideration. However, there is variation in optimal MDA implementation times for three and four MDA rounds. For a higher initial mosquito ratio, m_0, the optimal interval between MDA rounds is longer (Figs. 2C and D). Note that, with super-infection and seasonality in the mosquito population, a small number of initial mosquitoes can sustain a greater disease prevalence. We utilise these deterministic-model optimal timings in the stochastic model for up to four MDA rounds to study the impact of MDA with radical cure

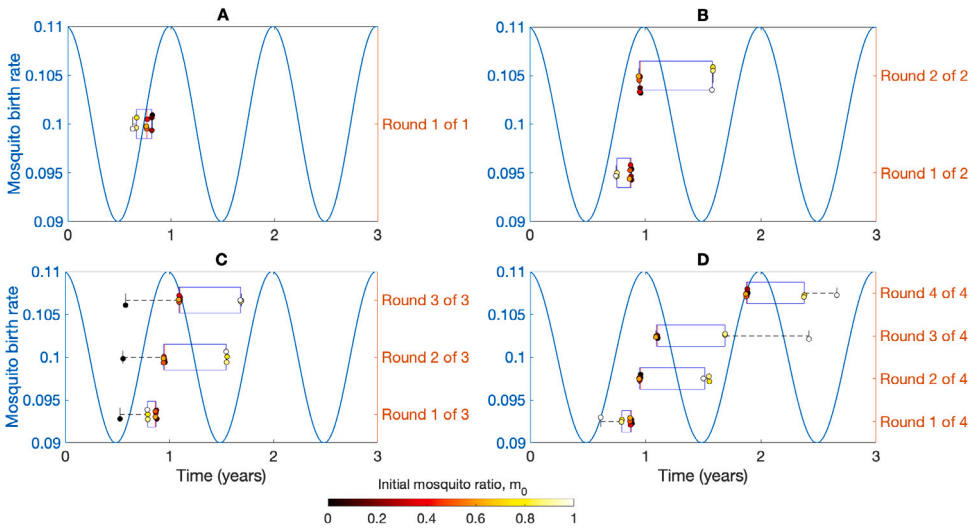

Fig. 2. Optimal MDA times for up to four rounds (right vertical axis) obtained with the deterministic version of the model in reference to seasonal mosquito birth rate $\theta(t)$ (left vertical axis). The box plot shows the distribution of the optimal MDA implementation times (see Table S1 for the optimal timings), whereas the coloured scattered points indicate the exact optimal time for different initial mosquito to human ratios. These different initial mosquito ratios correspond to prevalence of blood-stage infection in the range 10%–90%.

on *P. vivax* elimination. We also investigate another strategy referred to as "simplified MDA time", where we implement the first MDA round at a fixed time (after 5 years of burn-in). For this simplified approach the MDA rounds are implemented at 30 day intervals instead of the optimal. The optimal interval between the first and second rounds (x_1) when up to four rounds are under consideration, stays close to 29 days when prevalence is 20%–60% (see Table S1 and Figure S2 in Supplementary Material). Hence, we chose an interval of 30 days between all the rounds for the simplified approach. We compare the probability of elimination under this simplified strategy with the optimal strategies.

2.4. Model implementation

We initially obtain the optimal timing for MDA rounds using the deterministic version of the stochastic model. To efficiently simulate (approximate) trajectories from the stochastic model (see Algorithm 1), we use τ-leaping (Gillespie, 2001). We obtain the associated model quantities at equilibrium corresponding to a fixed prevalence using the steady-state analysis and initialise the population in the stochastic model at this state. Here, we use the mean-field approximation of the within-host model to obtain the time-dependent parameters $p(t)$, $p_1(t)$, $p_2(t)$, $k_1(t)$, and $k_T(t)$ which makes computation faster. The initial conditions, including mosquito to human ratio were chosen to have a prevalence of blood-stage infection in the range of 10%–90%, chosen to enable exploration of a wide range of prevalences. We used the MATLAB optimisation tool 'Multistart' with 50 different choices of initial starting points for the optimisation algorithm with *fmincon* (SQP algorithm) to generate global optimal solutions. All model parameters are described in Table 2. The optimisation model is implemented to start at year 5 to allow some burn-in period (we obtained the value of m_0 using the deterministic model to obtain the equilibrium mean prevalence of blood-stage infections for the stochastic model as described in Anwar et al. (2023a)).

Algorithm 1: Algorithm to approximate an exact trajectory of the stochastic model.

1 Define parameters. Choose $\tau = 1$ day. Initialise model with initial condition $\{S(0), I(0), L(0), S_m(0), E_m(0), I_m(0)\}$.
2 **while** $t < t_{end}$ *or* $I + L + E_m + I_m = 0$, **do**
3 Calculate the time-dependent parameters $p(t)$, $p_1(t)$, $p_2(t)$, $k_1(t)$, and $k_T(t)$ using Eqs. (6), (2), (3), (4), (5), respectively.
4 Calculate all the event rates R_j, $j = 1, 2, \ldots, 15$ as in Table 1.
5 For each event E_j, $j = 1, 2, \ldots, 15$ in Table 1, generate $K_j \sim \text{Poisson}(R_j\tau)$ that provides the number of each event that occurs within the time interval $[t,\ t + \tau]$.
6 Update the states $\{S, I, L, S_m, E_m, I_m\}$ at time $t + \tau$.

3. Results

We consider up to four rounds of MDA to study the impact of radical cure treatment on *P. vivax* elimination. Fig. 3 presents the impact of one and four rounds of MDA on the number of humans in the I and L compartments. Here, the timings of the MDA rounds (vertical lines) are chosen to be the optimal MDA times from the deterministic model when the initial mosquito to human ratio is $m_0 = 0.38$ (m_0 is chosen here to have a moderate transmission intensity (70% prevalence of blood-stage infections, see the steady-state analysis as per Anwar et al., 2023a)). Figs. 3A and C depict the effect of one MDA round, while Figs. 3B and D depict the effect of four MDA rounds on the number of humans in the I and L compartments, respectively. As we assume that the efficacy of the radical cure drug is 90%, the hypnozoite reservoir is never fully cleared when the drug is administered. Therefore, many individuals will transition to the L compartment, explaining the spikes in Figs. 3C and D when the first round of MDA is administered. Under four MDA rounds, the median trajectories for both infections reach close to zero (Figs. 3B, D) after the fourth round. However, new mosquito bites and hypnozoites from new bites, as well as those hypnozoites that survived the radical cure (because of imperfect drug efficacy), contribute to new infections. This drives the median trajectory for the number of blood-stage infections to eventually increase (Figs. 3A, B), albeit with high levels of uncertainty.

P. vivax transmission dynamics are primarily dominated by hypnozoite dynamics as an estimated 79%–96% of all *P. vivax* infections are due to relapse (in the absence of radical cure treatment) (Luxemburger et al., 1999; Baird, 2008; Betuela et al., 2012; Commons et al., 2018, 2019). Hence, even if the number of blood-stage infections reaches zero, the activation of hypnozoites can contribute to new blood-stage infections, re-initiating or sustaining transmission. Fig. 4 depicts the probability of elimination (green) and the probability of no blood-stage

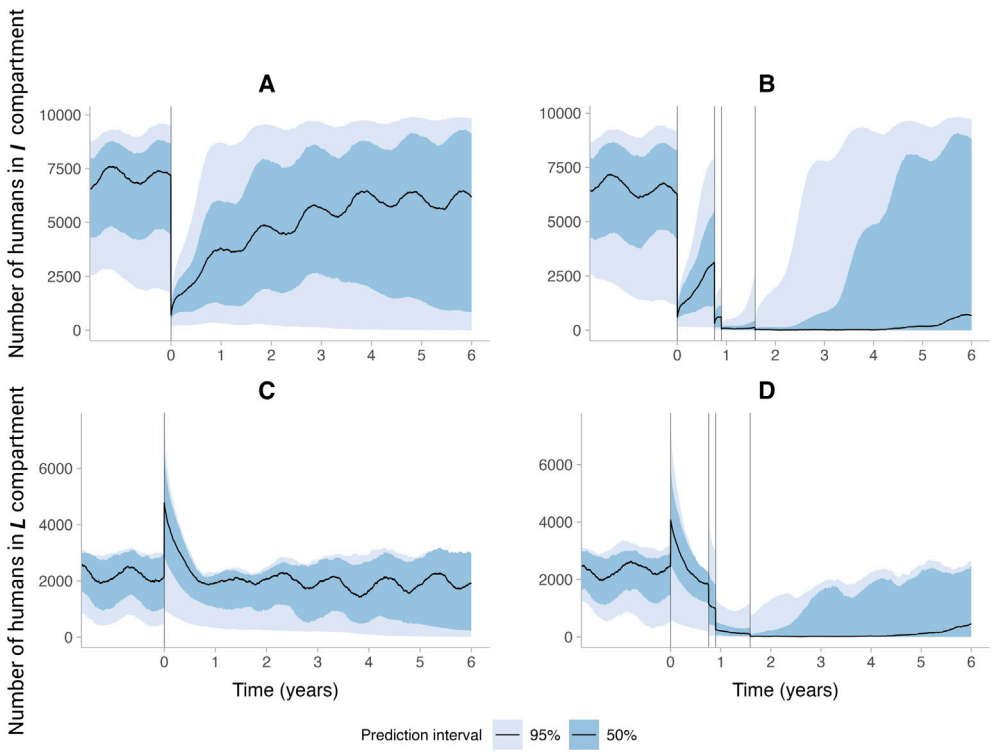

Fig. 3. Effect of one (first column) and four (second column) MDA rounds from 1000 simulations with $T_h = 10000$, $m_0 = 0.38$. Subplots A and C illustrate the effect of one MDA round on the number of humans in the I and L compartments, respectively. Subplots B and D illustrate the effect of four MDA rounds, respectively. The median trajectory out of the 1000 trajectories is indicated by the black line with 50% and 95% prediction intervals shown in shading. The grey vertical lines indicate the time of each MDA round. Parameters are as in Table 2.

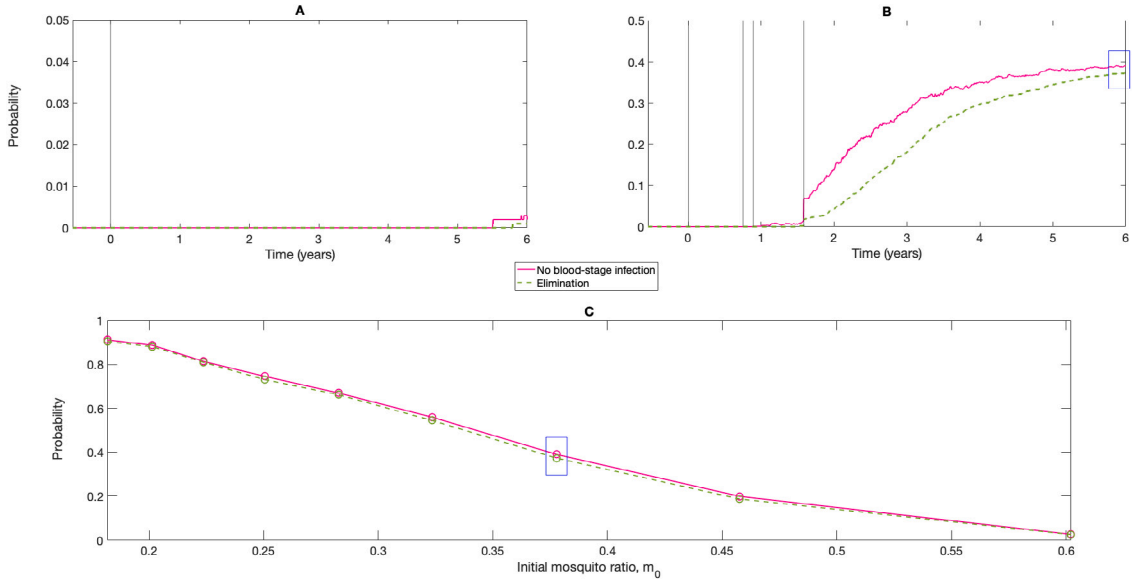

Fig. 4. Probability of *P. vivax* elimination (green) and probability of no blood-stage infection (magenta) over time under one (Subplot A) and four (Subplot B) MDA rounds, respectively, with the initial mosquito to human ratio, $m_0 = 0.38$. The probability of no blood-stage infection is estimated as the ratio of simulations where there are no blood-stage infections in the entire population (at the end of the simulation) from the 1000 simulations. The vertical lines indicate the MDA implementation times. Subplot C: Probability of *P. vivax* elimination and probability of no blood-stage infection for a varying number of initial mosquito to human ratios, m_0, under four MDA rounds. Probabilities are evaluated after six years from the first MDA round (from 1000 stochastic simulations). The blue box in Subplot C illustrates the evaluated probability in Subplot B. Note the different scales of the vertical axes in the subplots. Parameters are as in Table 2. (For interpretation of the references to colour in this figure legend, the reader is referred to the web version of this article.)

infection is estimated as the ratio of simulations where there are no blood-stage infections (at the end of the simulation) from the 1000 simulations. Figs. 4A and B depict the probability under one and four MDA rounds, respectively, when the initial mosquito to human ratio is $m_0 = 0.38$. The probability of elimination and the probability of no blood-stage infection under one MDA are very small (Fig. 4A). That is, one MDA round does not have any epidemiologically relevant effect on the probability of elimination when the transmission intensity

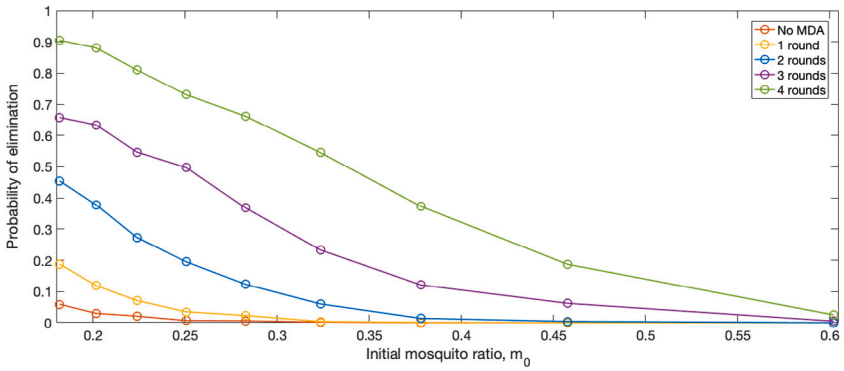

Fig. 5. Effect of up to four rounds of MDA on the probability of *P. vivax* elimination after six years with varying number of initial mosquito to human ratios, m_0, compared to no MDA (red line) from 1000 stochastic simulations. Parameters are as in Table 2. (For interpretation of the references to colour in this figure legend, the reader is referred to the web version of this article.)

is moderate to high (for the assumed human population size, $T_h = 10000$ and initial mosquito population size, $T_m = 3800$). However, the probability of elimination and the probability of no blood-stage infection under four MDA rounds increases over time after the fourth MDA round and is epidemiological relevant (in terms of magnitude), see Fig. 4B. Since we assume that any ongoing blood-stage infection will be cleared instantaneously due to the efficacy of the drug (here $p_{\text{blood}} = 0.9$), the number of blood-stage infections is driven down to very low numbers immediately following the fourth MDA round (as per Figs. 3B). The stochastic event of blood-stage elimination is more likely when blood-stage infection numbers are low, which explains why the probability of no blood-stage infection increases after the fourth MDA round. Furthermore, since we assume that hypnozoites in the liver are cleared instantaneously upon administration of the radical cure, the effect of radical cure on hypnozoites not only depends on the efficacy of the drug (here each hypnozoite is cleared with probability $p_{\text{rad}} = 0.9$) but also on the hypnozoite reservoir size (k_T). Activation of the hypnozoites that survive radical cure, and subsequent infectious mosquito bites, contribute to new blood-stage infections; thus the probability of no blood-stage infection over time is not monotonically increasing over time. This is distinct from the probability of elimination, which monotonically increases since elimination is an absorbing state of the system. The probability of elimination and the probability of no blood-stage infection vary across different transmission intensities. Fig. 4C depicts the probability of elimination and the probability of no blood-stage infection under four rounds of MDA for varying initial mosquito to human ratios, m_0, six years after the first MDA round. The lower the initial mosquito to human ratio, m_0, the higher the probabilities of elimination and no blood-stage infection. We note that these results are for a fixed human population size, $T_h = 10000$; the probability of elimination would vary with T_h.

The probabilities of *P. vivax* elimination after six years for up to four rounds of MDA, and no MDA, for varying initial mosquito to human ratios, m_0, are depicted in Fig. 5. The overall impact of one MDA round (yellow line, Fig. 5) is not substantially different compared to no MDA (red line, Fig. 5), particularly as the initial mosquito ratio (m_0) increases. When the initial mosquito to human ratio, m_0, is low, a small proportion of simulations fade out even if there are no rounds of MDA, which corresponds to a low probability of elimination. However, as the transmission intensity increases with increasing m_0, there is negligible probability of elimination without MDA. As m_0 increases, the probability of elimination decreases (regardless of MDA number and timing). Furthermore, the probability of elimination increases for fixed m_0 as the number of MDA rounds increases. That is, with a higher number of MDA rounds (and m_0 held fixed), the probability of *P. vivax* elimination is higher.

Hypnozoite dynamics and the efficacy of radical cure have a considerable influence on *P. vivax* transmission and elimination. Fig. 6 illustrates the sensitivity of the probability of *P. vivax* elimination to some key model parameters under four rounds of MDA for a fixed $m_0 = 0.38$. The initial mosquito to human ratio m_0 is chosen here to give a moderate transmission intensity and a moderate chance of *P. vivax* elimination after six years (see Fig. 4C). Note that the timing of the four MDA rounds is derived optimally (using the deterministic version of the model) for the baseline set of parameter values (vertical line in each subplot in Fig. 6) from Table 2. It is likely that the optimal timing would change as the model parameters under consideration here are varied, but we use the same timings to allow for direct comparisons. The stochastic variation evident in each subplot is due to the finite sample size (here 1000 model simulations were considered) used to compute Monte Carlo estimates for the probability of elimination. Fig. 6A depicts the probability of elimination over the hypnozoite activation rate, α, where the vertical line indicates the baseline rate as per Table 2. When the activation rate, α, is zero, the only option for the hypnozoite is to die. In such cases, infectious mosquitoes are the only driver of ongoing disease transmission. Hence, with four rounds of MDA, there is a high chance of eliminating *P. vivax* with a probability very close to one. However, as we have assumed that radical cure does not provide protection from new infections, the disease may re-establish. As the activation rate, α, increases from zero, relapse in addition to infectious bites contributes to onward transmission, and the probability of elimination decreases.

The probability of elimination as a function of the hypnozoite death rate, μ, under four rounds of MDA is depicted in Fig. 6B. If the hypnozoite death rate, μ, is zero, the hypnozoites can only activate, increasing the disease burden, resulting in a very low probability of elimination (due to stochasticity, some simulations still fade out). The probability of elimination increases as the hypnozoite death rate increases. That is, the higher the death rate, μ, the higher the chance of elimination, as with hypnozoites dying more frequently, the disease burden from relapse decreases. Figs. 6C–D depict the elimination probability for varying efficacy of the blood-stage and liver-stage drugs, respectively, when the other underlying parameters are as in Table 2. Unsurprisingly the probability of elimination increases with the efficacy of the blood-stage clearance drug and is the highest when 100% effective. The reason that the probability of elimination is not 100% when the blood-stage drug is 100% effective is that the effectiveness of the liver-stage clearance drug, p_{rad}, is set at the baseline value of 90%. Since it is possible that hypnozoites are not fully cleared, in addition to subsequent infectious mosquito bites, relapses can re-establish transmission. In the case of liver-stage drugs, the probability of elimination also increases with the efficacy of the liver-stage clearance drug, p_{rad}. Again, the more effective the drugs are, the higher the probability of elimination, peaking when 100% effective. It is worth noting that, radical cure with a low-efficacy drug, especially the liver-stage clearance drug, has little to no effect. That is, the chances of elimination improve with high-efficacy drugs.

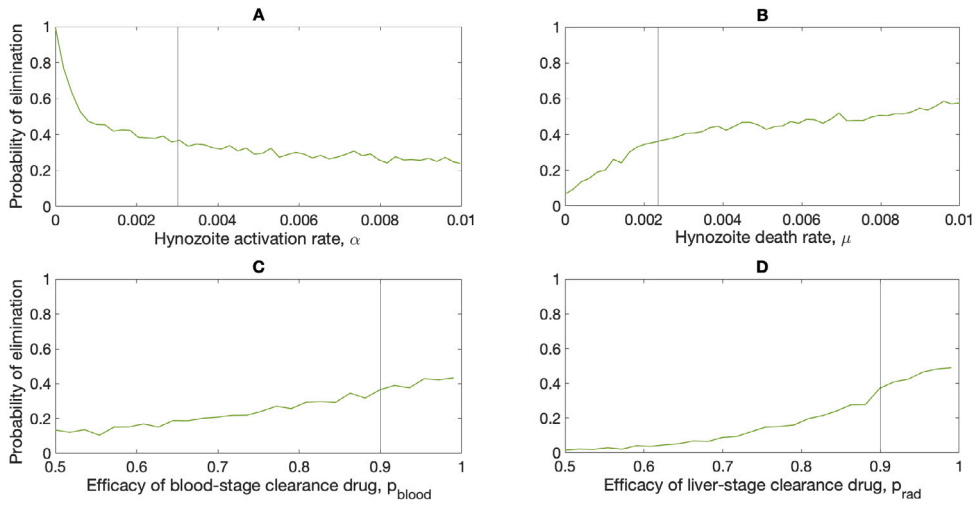

Fig. 6. Sensitivity of probability of *P. vivax* elimination after six years over key model parameters under four rounds of MDA from 1000 stochastic simulations. Subplots A–D depict the probability of elimination over hypnozoite activation rate, α, hypnozoite death rate, μ, the efficacy of blood-stage clearance drug, p_{blood}, and the efficacy of liver-stage clearance drug, p_{rad}, respectively. The vertical line in each subplot indicates the baseline parameters used throughout Figs. 2–5. Probabilities are evaluated after six years from the first MDA round. All other parameters are as in Table 2.

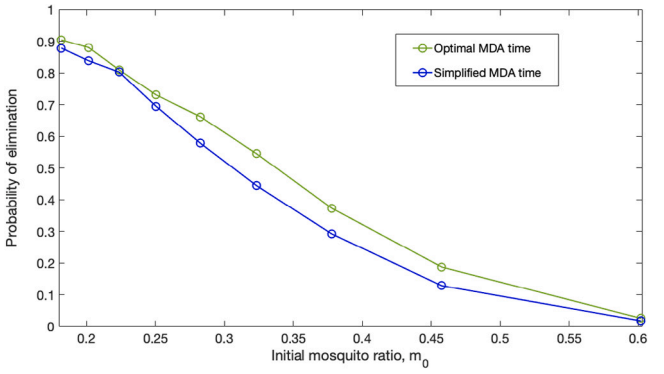

Fig. 7. Probability of *P. vivax* elimination under four rounds of MDA with optimal timing (green line, timings of MDA decided as per the deterministic version of the model) compared to simplified MDA timing (blue solid line) for varying m_0 with 1000 simulations. Probabilities are evaluated at year six from the first MDA round. All other parameters are as in Table 2. (For interpretation of the references to colour in this figure legend, the reader is referred to the web version of this article.)

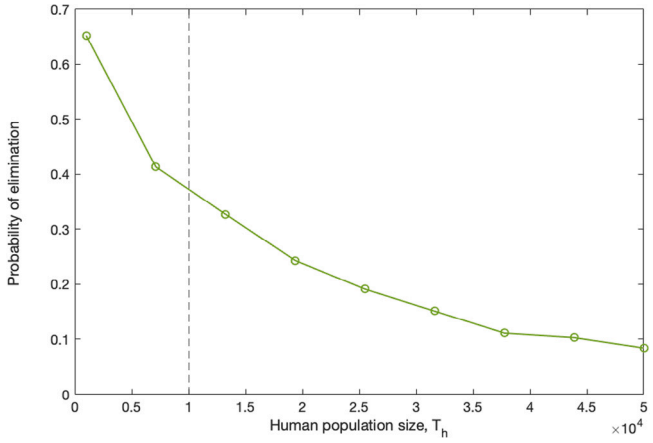

Fig. 8. Sensitivity of probability of *P. vivax* elimination after six years as total human population size, T_h, varies (with four MDA rounds), with the initial mosquito to human ratio, $m_0 = 0.38$. The vertical line represents the baseline population size. All other parameters are as in Table 2.

We explored how much the specific timing for MDA implementation affects the probability of *P. vivax* elimination. To illustrate this, we use a simplified way of implementing four MDA rounds. Namely, we implement the MDA rounds with a 30 day interval instead of the optimal intervals (as determined using a deterministic analysis). We note that the choice of this 30 day interval is influenced by the optimal intervals as discussed in Section 2.3. Fig. 7 illustrates the probability of elimination under four MDA rounds with the optimal timing (green line) and compares to the simplified timing (blue line) for varying values of the initial mosquito to human ratio, m_0. Here, for every choice of the initial mosquito to human ratio, m_0, the optimal approach (as determined using the deterministic model) provides better results in terms of yielding a higher probability of elimination. However, the differences are not substantial and depending on other potential factors, policymakers could also consider a simplified strategy based on resources.

The stochastic effect of disease elimination is more evident when the population size is small. That is, due to stochasticity, the probability of elimination would be higher, even without any MDA rounds with a low population size. Fig. 8 illustrates the sensitivity analysis of the probability of *P. vivax* elimination over the population size, T_h under four rounds of MDA, with the initial mosquito to human ratio, $m_0 = 0.38$. The probability of *P. vivax* elimination is high when the population size is low and decreases as the population size increases.

4. Discussion

As *P. vivax* transmission is primarily dominated by hypnozoite dynamics, targeting the hypnozoites with a radical cure to disrupt transmission is crucial to achieve the goal of *P. vivax* elimination (Anwar et al., 2023a; Nekkab et al., 2023). In this article, we study the impact of multiple rounds of MDA with radical cure on *P. vivax* elimination, defined to be when there are no infections in both human and mosquito populations. We previously studied the optimal interruption of *P. vivax* transmission with MDA under a deterministic multiscale model (see Anwar et al., 2023a), but since this model was developed in a deterministic framework, disease elimination was not able to be considered. Here we have implemented a stochastic model to allow us to investigate elimination. We evaluate the probability of *P. vivax* elimination after six years from the first MDA, which has been chosen to fit with the current public health goals to achieve malaria

elimination in at least 35 countries by 2030 according to WHO's Global Technical Strategy (Mberikunashe et al., 2021). We observed that, as expected, the more MDA rounds there are, the better the chance of *P. vivax* elimination (Fig. 5). The administration times of the MDA rounds, when multiple MDA rounds are under consideration, can affect the probability of elimination (Fig. 7). Our results demonstrate that reductions in transmission due to MDA would likely be short-lived (unless elimination is achieved) as the underlying driver of transmission (infectious mosquitoes) remains unchanged by the intervention. As the abundance of mosquitoes greatly affects *P. vivax* dynamics, the higher the mosquito population sizes are, the lower the probability of elimination (results not explicitly shown here), regardless of how many MDA rounds are considered, up to the four we explored (Fig. 5). This is also true for the human population size (Fig. 8). We also observed that it is important to consider a radical cure with high efficacy (Fig. 6D). Otherwise, the impact of MDA rounds on *P. vivax* elimination probability could be limited (this also depends on other model parameters). However, even with highly effective drugs and varying numbers of MDA rounds, elimination is anticipated to be unlikely with MDA alone (for example, the probability of elimination does not reach 100% for any parameter combinations considered in Fig. 6).

The possibility of *P. vivax* elimination under MDA depends on many different factors, for example, how effective the drugs are and what proportion of the population is covered under MDA (Asih et al., 2018; Thriemer et al., 2021). In this work, we assumed that radical cure drugs are 90% effective in clearing both blood-stage parasites and hypnozoites, which approximates the high end of the estimated efficacy region of 87·2–89·9% for tafenoquine (recurrence-free effectiveness until day 90) (Brito et al., 2024). Since we explicitly model the impact of radical cure drugs on both blood-stage infections and hypnozoite dynamics, for model simplicity, we assumed 100% treatment coverage in our model, which is difficult to achieve in reality due to various factors (Agboraw et al., 2021; Finn et al., 2020). Note that, to consider a lower MDA coverage, a different model framework would be required that allows the hypnozoite distribution to be kept track of separately in individuals that receive treatment and those who do not. We do not consider drug prophylaxis and drug adherence in our model. Accounting for prophylaxis might vary model outcomes, as a longer duration of prophylaxis leads to greater measured efficacy, especially in higher transmission settings (Huber et al., 2021). Furthermore, given the mosquito has a shorter lifespan, for a longer duration of prophylaxis, a reasonable proportion of infectious mosquitoes may die out and disrupt the chains of transmission. We accounted for the seasonal transmission setting in our model through the mosquito birth rate by changing the amplitude of transmission intensity. Additionally, an extended rainy and a shorter summer season would keep the transmission intensity higher for a longer duration, which would lower the probability of elimination. Furthermore, human and mosquito movement in and out of the study area may also result in the potential reintroduction of infection, which we did not consider (Das et al., 2023), though reactivation still results in a type of reintroduction into the target population. This means that, in regards to this parameter, our results are optimistic: our model's estimate of the probability of elimination is an upper bound. Furthermore, because of the risk of hemolysis in G6PD–deficient individuals, radical cure is not recommended by the WHO without screening for G6PD deficiency (WHO, 2021; Howes et al., 2012; Watson et al., 2018). Currently, we do not consider G6PD deficiency in our model. Therefore, accounting for G6PD deficiency is a potential avenue for future work and accounting for it will reduce the probability of elimination since fewer people will be able to take radical cure drugs.

Furthermore, because of the extensive use of antimalarial drugs, the *P. vivax* parasite has developed resistance to some drugs, particularly chloroquine which is another reason MDA is not recommended. *P. vivax* resistance to antimalarial drugs, including chloroquine, mefloquine, sulfadoxine, and pyrimethamine, has been reported in many parts of the world (Battle et al., 2019). However, chloroquine is still effective in most parts of the world for *P. vivax* (WHO, 2023b). We currently do not consider drug resistance in our model. Moreover, the role of immunity can greatly influence how malaria dynamics progress through the population. However, we do not consider immunity. Individuals who have not previously experienced malaria infection almost invariably become infected when first exposed to infectious mosquito bites, as immunity against malaria has not yet developed (Langhorne et al., 2008). Repeated exposure to infectious bites will still likely result in infection, though these individuals may be protected against severe malaria or death (Langhorne et al., 2008). However, the immunity acquired from a primary infection may protect more strongly against relapses (which are genetically related to the primary infection) than against a new, genetically distinct primary infection (Anwar et al., 2023b). This is because the parasites could be genetically identical or related, which could elicit a more protective immune response due to familiarity with the primary infection (White, 2011; Joyner et al., 2019). Thus, relapses from the same batch of hypnozoites may be more likely only to cause asymptomatic infections. Since the multi-scale model presented here depends on the history of past infections, including the role of immunity is, therefore, a potential future work as immunity against *P. vivax* strongly correlates to past infections.

From a methodological perspective, another limitation of our work is that we utilised the optimal MDA implementation times from a deterministic analysis of the stochastic version of the model. We also have not calibrated our model to any data, and only conducted one-dimensional sensitivity analyses. To further identify model parameters which have the greatest impact on model outcome, a multi-dimensional sensitivity analysis (such as LHS-PRCC) is required. Therefore, all these are fruitful avenues for future work.

Mosquito dynamics greatly influence *P. vivax* dynamics, and as such, vector interventions, for example, long-lasting insecticide nets (LLIN) and indoor residual spray (IRS), should be considered along with MDA. Although we do not explicitly consider vector interventions in this paper, in areas where vector interventions are applied consistently, they can be implicitly considered through m_0 by assuming an overall (constant) effect on the mosquito population (see Fig. 7). We note there have been substantial efforts invested in explicitly exploring mosquito interventions (White et al., 2014, 2018; Nekkab et al., 2021). The primary purpose of this work was to study the impact of MDA on *P. vivax* elimination; hence, studying the impact of MDAs along with other vector interventions is left for future work. Nonetheless, as our model accounts for stochasticity and hypnozoite dynamics in more detail, and we model the impact of MDA on each hypnozoite and blood-stage infection independently, our research has the potential to contribute towards the goal of *P. vivax* elimination.

CRediT authorship contribution statement

Md Nurul Anwar: Writing – review & editing, Writing – original draft, Visualization, Validation, Methodology, Investigation, Formal analysis, Conceptualization. **James M. McCaw:** Writing – review & editing, Supervision. **Alexander E. Zarebski:** Writing – review & editing. **Roslyn I. Hickson:** Writing – review & editing, Supervision, Conceptualization. **Jennifer A. Flegg:** Writing – review & editing, Supervision, Conceptualization.

Declaration of competing interest

The authors declare that they have no known competing financial interests or personal relationships that could have appeared to influence the work reported in this paper.

Acknowledgements

This research was supported by The University of Melbourne's Research Computing Services and the Petascale Campus Initiative, Australia. J.A. Flegg's research is supported by the Australian Research Council, Australia (DP200100747, FT210100034) and the National Health and Medical Research Council, Australia (APP2019093). J.M. McCaw's research is supported by the Australian Research Council, Australia (DP210101920) and the NHMRC Australian Centre of Research Excellence in Malaria Elimination (ACREME) (APP1134989). The contents of the published material are solely the responsibility of the individual authors and do not reflect the views of NHMRC.

Appendix A. Supplementary data

Supplementary material related to this article can be found online at https://doi.org/10.1016/j.epidem.2024.100789.

References

Agboraw, Efundem, Sosu, Fred, Dean, Laura, Siakeh, Alice, Thomson, Rachael, Kollie, Karsor, Worrall, Eve, 2021. Factors influencing mass drug administration adherence and community drug distributor opportunity costs in Liberia: A mixed-methods approach. Parasites Vectors 14, 1–11.

Allen, Linda J.S., Burgin, Amy M., 2000. Comparison of deterministic and stochastic SIS and SIR models in discrete time. Math. Biosci. 163 (1), 1–33.

Antinori, Spinello, Galimberti, Laura, Milazzo, Laura, Corbellino, Mario, 2012. Biology of human malaria plasmodia including Plasmodium knowlesi. Mediterr. J. Hematol. Infect. Dis. 4 (1).

Anwar, Md Nurul, Hickson, Roslyn I., Mehra, Somya, McCaw, James M., Flegg, Jennifer A., 2022. A multiscale mathematical model of Plasmodium vivax transmission. Bull. Math. Biol. 84 (8), 1–24.

Anwar, Md Nurul, Hickson, Roslyn I., Mehra, Somya, Price, David J., McCaw, James M., Flegg, Mark B., Flegg, Jennifer A., 2023a. Optimal interruption of P. vivax malaria transmission using mass drug administration. Bull. Math. Biol. 85 (6), 43.

Anwar, Md Nurul, Smith, Lauren, Devine, Angela, Mehra, Somya, Walker, Camelia R., Ivory, Elizabeth, Conway, Eamon, Mueller, Ivo, McCaw, James M., Flegg, Jennifer A., et al., 2023b. A scoping review of mathematical models of plasmodium vivax. arXiv preprint arXiv:2309.00274.

Asih, Puji B.S., Syafruddin, Din, Baird, John Kevin, 2018. Challenges in the control and elimination of Plasmodium vivax malaria. Towards Malar. Elimin. A Leap Forw. 77.

Baird, J. Kevin, 2008. Real-world therapies and the problem of vivax malaria. N. Engl. J. Med. 359 (24), 2601–2603.

Battle, Katherine E., Lucas, Tim C.D., Nguyen, Michele, Howes, Rosalind E., Nandi, Anita K., Twohig, Katherine A., Pfeffer, Daniel A., Cameron, Ewan, Rao, Puja C., Casey, Daniel, et al., 2019. Mapping the global endemicity and clinical burden of Plasmodium vivax, 2000–17: A spatial and temporal modelling study. Lancet 394 (10195), 332–343.

Beran, Jan, 1994. Statistics for Long-Memory Processes, vol. 61. CRC Press.

Betuela, Inoni, Rosanas-Urgell, Anna, Kiniboro, Benson, Stanisic, Danielle I., Samol, Lornah, de Lazzari, Elisa, del Portillo, Hernando A., Siba, Peter, Alonso, Pedro L., Bassat, Quique, et al., 2012. Relapses contribute significantly to the risk of plasmodium vivax infection and disease in papua new guinean children 1–5 years of age. J. Infect. Dis. 206 (11), 1771–1780.

Bharti, Ajay R., Chuquiyauri, Raul, Brouwer, Kimberly C., Stancil, Jeffrey, Lin, Jessica, Llanos-Cuentas, Alejandro, Vinetz, Joseph M., 2006. Experimental infection of the neotropical malaria vector anopheles darlingi by human patient-derived plasmodium vivax in the peruvian Amazon. Am. J. Trop. Med. Hyg. 75 (4), 610–616.

Brito, Marcelo, Rufatto, Rosilene, Brito-Sousa, José Diego, Murta, Felipe, Sampaio, Vanderson, Balieiro, Patrícia, Baía-Silva, Djane, Castro, Vanessa, Alves, Brenda, Alencar, Aline, et al., 2024. Operational effectiveness of tafenoquine and primaquine for the prevention of plasmodium vivax recurrence in Brazil: A retrospective observational study. Lancet Infect. Dis. 24 (6), 629–638.

Collins, William E., Jeffery, Geoffrey M., Roberts, Jacquelin M., 2003. A retrospective examination of anemia during infection of humans with plasmodium vivax. Am. J. Trop. Med. Hyg. 68 (4), 410–412.

Commons, Robert J., Simpson, Julie A., Thriemer, Kamala, Hossain, Mohammad S., Douglas, Nicholas M., Humphreys, Georgina S., Sibley, Carol H., Guerin, Philippe J., Price, Ric N., 2019. Risk of Plasmodium vivax parasitaemia after Plasmodium falciparum infection: A systematic review and meta-analysis. Lancet Infect. Dis. 19 (1), 91–101.

Commons, Robert J., Simpson, Julie A., Thriemer, Kamala, Humphreys, Georgina S., Abreha, Tesfay, Alemu, Sisay G., Añez, Arletta, Anstey, Nicholas M., Awab, Ghulam R., Baird, J. Kevin, et al., 2018. The effect of chloroquine dose and primaquine on Plasmodium vivax recurrence: A WorldWide Antimalarial Resistance Network systematic review and individual patient pooled meta-analysis. Lancet Infect. Dis. 18 (9), 1025–1034.

Das, Aatreyee M., Hetzel, Manuel W., Yukich, Joshua O., Stuck, Logan, Fakih, Bakar S., Al-Mafazy, Abdul-Wahid H., Ali, Abdullah, Chitnis, Nakul, 2023. Modelling the impact of interventions on imported, introduced and indigenous malaria infections in Zanzibar, Tanzania. Nature Commun. 14 (1), 2750.

Finn, Timothy P., Yukich, Joshua O., Bennett, Adam, Porter, Travis R., Lungu, Christopher, Hamainza, Busiku, Kawesha, Elizabeth Chizema, Conner, Ruben O., Silumbe, Kafula, Steketee, Richard W., et al., 2020. Treatment coverage estimation for mass drug administration for malaria with dihydroartemisinin–piperaquine in Southern province, zambia. Am. J. Trop. Med. Hyg. 103 (2 Suppl), 19.

Garrett-Jones, C., 1964. The human blood index of malaria vectors in relation to epidemiological assessment. Bull. World Health Organ. 30 (2), 241.

Gething, Peter W., Van Boeckel, Thomas P., Smith, David L., Guerra, Carlos A., Patil, Anand P., Snow, Robert W., Hay, Simon I., 2011. Modelling the global constraints of temperature on transmission of plasmodium falciparum and P. vivax. Parasites Vectors 4 (1), 92.

Ghosh, Mini, Olaniyi, Samson, Obabiyi, Olawale S., 2020. Mathematical analysis of reinfection and relapse in malaria dynamics. Appl. Math. Comput. 373, 125044.

Gillespie, Daniel T., 2001. Approximate accelerated stochastic simulation of chemically reacting systems. J. Chem. Phys. 115 (4), 1716–1733.

Henle, Klaus, Sarre, Stephen, Wiegand, Kerstin, 2004. The role of density regulation in extinction processes and population viability analysis. Biodivers. Conserv. 13 (1), 9–52.

Howes, Rosalind E., Piel, Frederic B., Patil, Anand P., Nyangiri, Oscar A., Gething, Peter W., Dewi, Mewahyu, Hogg, Mariana M., Battle, Katherine E., Padilla, Carmencita D., Baird, J. Kevin, et al., 2012. G6PD deficiency prevalence and estimates of affected populations in malaria endemic countries: A geostatistical model-based map. PLoS Med. 9 (11).

Hsiang, Michelle S., Hwang, Jimee, Tao, Amy R., Liu, Yaobao, Bennett, Adam, Shanks, George Dennis, Cao, Jun, Kachur, Stephen Patrick, Feachem, Richard G.A., Gosling, Roly D., et al., 2013. Mass drug administration for the control and elimination of plasmodium vivax malaria: An ecological study from Jiangsu province, China. Malar. J. 12 (1), 1–14.

Huber, John H., Koepfli, Cristian, España, Guido, Nekkab, Narimane, White, Michael T., Alex Perkins, T., 2021. How radical is radical cure? Site-specific biases in clinical trials underestimate the effect of radical cure on Plasmodium vivax hypnozoites. Malar. J. 20 (1), 1–15.

Hulden, Lena, Hulden, Larry, 2011. Activation of the hypnozoite: A part of plasmodium vivax life cycle and survival. Malar. J. 10 (1), 90.

Imwong, Mallika, Snounou, Georges, Pukrittayakamee, Sasithon, Tanomsing, Naowarat, Kim, Jung Ryong, Nandy, Amitab, Guthmann, Jean-Paul, Nosten, Francois, Carlton, Jane, Looareesuwan, Sornchai, et al., 2007. Relapses of Plasmodium vivax infection usually result from activation of heterologous hypnozoites. J. Infect. Dis. 195 (7), 927–933.

Joyner, Chester J., Brito, Cristiana F.A., Saney, Celia L., Joice Cordy, Regina, Smith, Maren L., Lapp, Stacey A., Cabrera-Mora, Monica, Kyu, Shuya, Lackman, Nicolas, Nural, Mustafa V., et al., 2019. Humoral immunity prevents clinical malaria during Plasmodium relapses without eliminating gametocytes. PLoS Pathog. 15 (9), e1007974.

Kurtz, Thomas G., 1970. Solutions of ordinary differential equations as limits of pure jump Markov processes. J. Appl. Probab. 7 (1), 49–58.

Langhorne, Jean, Ndungu, Francis M., Sponaas, Anne-Marit, Marsh, Kevin, 2008. Immunity to malaria: More questions than answers. Nature Immunol. 9 (7), 725–732.

Ludwig, Donald, 1999. Is it meaningful to estimate a probability of extinction? Ecology 80 (1), 298–310.

Luxemburger, Christine, van Vugt, Michèle, Jonathan, Saw, McGready, Rose, Looareesuwan, Sornchai, White, Nicholas J., Nosten, François, 1999. Treatment of vivax malaria on the western border of Thailand. Trans. R. Soc. Trop. Med. Hyg. 93 (4), 433–438.

Mberikunashe, Joseph, Chisanga, Brian, Menale, Kassie, Chanda10, Emmanuel, Mutero, Clifford Maina, 2021. Onyango p. Sangoro1, ulrike fillinger1, kochelani saili1, 2, theresia estomih nkya1, rose marubu1, freddie masaninga3, sonia casimiro trigo4, casper tarumbwa5, busiku hamainza6, candrinho Baltazar7.

Mehra, Somya, Stadler, Eva, Khoury, David, McCaw, James M., Flegg, Jennifer A., 2022. Hypnozoite dynamics for Plasmodium vivax malaria: The epidemiological effects of radical cure. J. Theoret. Biol. 111014.

Mueller, Ivo, Galinski, Mary R., Baird, J. Kevin, Carlton, Jane M., Kochar, Dhanpat K., Alonso, Pedro L., del Portillo, Hernando A., 2009. Key gaps in the knowledge of Plasmodium vivax, a neglected human malaria parasite. Lancet Infect. Dis. 9 (9), 555–566.

Nekkab, Narimane, Lana, Raquel, Lacerda, Marcus, Obadia, Thomas, Siqueira, André, Monteiro, Wuelton, Villela, Daniel, Mueller, Ivo, White, Michael, 2021. Estimated impact of tafenoquine for Plasmodium vivax control and elimination in Brazil: A modelling study. PLoS Med. 18 (4), e1003535.

Nekkab, Narimane, Obadia, Thomas, Monteiro, Wuelton M., Lacerda, Marcus V.G., White, Michael, Mueller, Ivo, 2023. Accelerating towards P. vivax elimination with a novel serological test-and-treat strategy: A modelling case study in Brazil. Lancet Regional Health Am. 22.

Newby, Gretchen, Hwang, Jimee, Koita, Kadiatou, Chen, Ingrid, Greenwood, Brian, Von Seidlein, Lorenz, Shanks, G. Dennis, Slutsker, Laurence, Kachur, S. Patrick, Wegbreit, Jennifer, et al., 2015. Review of mass drug administration for malaria and its operational challenges. Am. J. Trop. Med. Hyg. 93 (1), 125.

Poespoprodjo, Jeanne Rini, Burdam, Faustina Helena, Candrawati, Freis, Ley, Benedikt, Meagher, Niamh, Kenangalem, Enny, Indrawanti, Ratni, Trianty, Leily, Thriemer, Kamala, Price, David J, et al., 2022. Supervised versus unsupervised primaquine radical cure for the treatment of falciparum and vivax malaria in Papua, Indonesia: A cluster-randomised, controlled, open-label superiority trial. Lancet Infect. Dis. 22 (3), 367–376.

Recht, Judith, Ashley, Elizabeth A., White, Nicholas J., 2018. Use of primaquine and glucose-6-phosphate dehydrogenase deficiency testing: Divergent policies and practices in malaria endemic countries. PLoS Negl. Trop. Dis. 12 (4), e0006230.

Robinson, Leanne J., Wampfler, Rahel, Betuela, Inoni, Karl, Stephan, White, Michael T., Suen, Connie S.N/ Li Wai, Hofmann, Natalie E., Kinboro, Benson, Waltmann, Andreea, Brewster, Jessica, et al., 2015. Strategies for understanding and reducing the plasmodium vivax and plasmodium ovale hypnozoite reservoir in Papua New Guinean children: A randomised placebo-controlled trial and mathematical model. PLoS Med. 12 (10), e1001891.

Smith, David L., Drakeley, Chris J., Chiyaka, Christinah, Hay, Simon I., 2010. A quantitative analysis of transmission efficiency versus intensity for malaria. Nature Commun. 1 (1), 1–9.

Taylor, Walter R.J., Thriemer, Kamala, von Seidlein, Lorenz, Yuentrakul, Prayoon, Assawariyathipat, Thanawat, Assefa, Ashenafi, Auburn, Sarah, Chand, Krisin, Chau, Nguyen Hoang, Cheah, Phaik Yeong, et al., 2019. Short-course primaquine for the radical cure of Plasmodium vivax malaria: A multicentre, randomised, placebo-controlled non-inferiority trial. Lancet 394 (10202), 929–938.

Thriemer, Kamala, Ley, Benedikt, von Seidlein, Lorenz, 2021. Towards the elimination of Plasmodium vivax malaria: Implementing the radical cure. PLoS Med. 18 (4), e1003494.

Watson, James, Taylor, Walter R.J., Bancone, Germana, Chu, Cindy S., Jittamala, Podjanee, White, Nicholas J., 2018. Implications of current therapeutic restrictions for primaquine and tafenoquine in the radical cure of vivax malaria. PLoS Negl. Trop. Dis. 12 (4), e0006440.

Wells, Timothy N.C., Burrows, Jeremy N., Baird, J. Kevin, 2010. Targeting the hypnozoite reservoir of Plasmodium vivax: The hidden obstacle to malaria elimination. Trends Parasitol. 26 (3), 145–151.

White, Nicholas J., 2011. Determinants of relapse periodicity in plasmodium vivax malaria. Malar. J. 10 (1), 297.

White, Michael T., Karl, Stephan, Battle, Katherine E., Hay, Simon I., Mueller, Ivo, Ghani, Azra C., 2014. Modelling the contribution of the hypnozoite reservoir to Plasmodium vivax transmission. eLife 3, e04692.

White, Michael T., Walker, Patrick, Karl, Stephan, Hetzel, Manuel W., Freeman, Tim, Waltmann, Andreea, Laman, Moses, Robinson, Leanne J., Ghani, Azra, Mueller, Ivo, 2018. Mathematical modelling of the impact of expanding levels of malaria control interventions on Plasmodium vivax. Nature Commun. 9 (1), 1–10.

WHO, 2021. Second Focused Review Meeting of the Malaria Elimination Oversight Committee (MEOC): Report of a Virtual Meeting, 28 June–1 July 2021. World Health Organization.

WHO, 2023a. Consolidated guidelines for malaria. https://www.who.int/teams/global-malaria-programme/guidelines-for-malaria (Accessed 10 May 2023).

WHO, 2023b. Tackling antimalarial drug resistance. https://www.who.int/news/item/18-11-2022-tackling-emerging-antimalarial-drug-resistance-in-africa. (Accessed 10 May 2023).